

Tests of R/C Beam-Column Joint with Variant Boundary Conditions and Irregular Details on Anchorage of Beam Bars

F. Kusuhara¹ and H. Shiohara²

¹ Assistant Professor, Dept. of Architecture, School of Engineering, The Univ. of Tokyo, Tokyo, Japan

² Associate Professor, Dept. of Architecture, School of Engineering, The Univ. of Tokyo, Tokyo, Japan

Email: kusuhara@rcs.arch.t.u-tokyo.ac.jp, shiohara@rcs.arch.t.u-tokyo.ac.jp

ABSTRACT :

Ten half-scale reinforced concrete beam-column joint sub-assemblages were loaded to failure by statically cyclic loading simulating earthquake loading, to obtain fundamental data including stress in bars after yielding and joint deformation. The test parameters were (1) boundary conditions and loading types for specimens with identical form, section and bar arrangement, (2) the forms of specimens with identical boundary condition and loading type, (3) with or without transverse beams and (4) details on anchorage of beam bars in interior and exterior joints. The test results indicated that (1) in some case of damage of joints were severe, maximum story shear were lower than predicted story shear at ultimate strength of beam in spite of beam bars were yielded, (2) the rotations of four parts of the joint divided with diagonal cracks were dominant in story drift deformation in case of joint failure after yielding of beams, (3) in case of damage of joints were severe, bond actions of beam bars or column bars passing through the joints kept low level and (4) poor anchorage length of beam bars in exterior joints led lower story shear capacity, yielding of column bars and severe damage in the joints.

KEYWORDS: reinforced concrete, beam-column joint, subcomponent of deformation, yield strength

1. INTRODUCTION

The major problem in the seismic design of RC beam-column joint is the lack of theory, which can explain the effect of the parameters which affect the strength, ductility and failure mode, of the beam-column joint subjected to high seismic force demand. Several theories have been recently proposed by researchers including one of the authors. For development and experimental verification of the theory, we have carried out series of tests on reinforced concrete beam-column sub-assemblages.

2. TEST PROGRAM

2.1. Specimens and Design Parameter

Ten half-scale reinforced concrete beam-column joint sub-assemblages were constructed. They were loaded by displacement control to failure under quasi-statically reversed cyclic load with increasing amplitudes simulating seismic loading condition. The specimens are beam-column joint sub-assemblages virtually isolated in moment resisting frame at contra-flexure point by substituting them by pin joints or pin-roller joints to simulate the stress condition in typical moment resisting frames.

The test program consists of five series of tests. Table 1 lists the specimens and their test parameters and Fig. 1 shows the geometry and the reinforcing details of the specimens. The cross sections of the beams are 300 x 300 mm and that of the columns are 300 x 300 mm in all the specimens. The width of the beams and the columns is identical so that the test result should not be affected by the effects of three-dimensional geometry. Three sets of hoops of D6 were placed in the beam-column joints in all the specimens; the amount of joint shear reinforcement is 0.3 %, which is the minimum requirement of the AIJ Guidelines.

Test series A consists of three plane beam-column joint specimens with the identical dimension, geometry, reinforcing arrangement and materials. All of them are of crucial form; two columns and beams are framing into one joint without transverse beam nor slab. Each of them is subject to one of three loading types described in loading setup. Specimen A1 simulated the condition of an interior beam-column joint (loading type I) and Specimen A2 and specimen A3 simulated the conditions of an exterior joint (loading type II) and a corner joint (loading type III) respectively. Amount of beam bars were chosen so that the joint shear demand is as high as possible within the allowable for joint shear stress specified in the AIJ Guidelines and the specimens were designed such that yielding moment capacity of column is 32 percent higher than that of the beam in case of tested by the condition of interior joints.

Test series B consists of two plane beam-column joint specimens of two different configurations without transverse beam nor slab. Specimen B1 is of crucial form, whereas specimen B2 is not crucial form; two columns and one beam are framed into one joint. Both of them were subjected to identical loading pattern of loading type II which simulated exterior beam-column joints. Amount of beam bars were chosen so that the joint shear demand is as high as possible within the allowable for joint shear stress specified in the AIJ Guidelines and the specimens were designed so that sum of ultimate moment capacities of the columns is 24 percent higher than the ultimate moment capacity of one beam.

Test series C comprises of only one specimen identical to Specimen A1 of crucial form, except it has transverse beams to simulate a beam-column joint with confinement of them. To simulate of the flexural cracks at the transverse beam ends, concrete gaps with 1.0 mm width were made at the column face. The specimen is subjected to identical loading pattern of Specimen A1.

Test series D consists of two plane beam-column joint specimens of crucial form, and one has anchor plates on middle of the beam bars in the beam-column joint and the other has bars passing the joint without special details. The diameter of beam bars is larger than that of the Specimens A1 and C1 and amount of beam bars were chosen so that the joint shear demand is 85 percent of allowable joint shear stress.

Test series E consists of two plane exterior beam-column joint specimens and the beam bars are headed with steel plate welded at the ends of bars. The difference between the two specimens is anchorage length, 86% and 53% of column depth respectively. Reinforcing arrangement of the beams is identical to that of test series D and the column bars were reduced to make the sum of ultimate moment capacities of the columns is 1.4 times higher than the ultimate capacity of the beam.

Table 1 List of specimens

	A1	A2	A3	C1	D1	D2	B1	B2	E1	E2	
form	+	+	+	+	+	+	+	┌	┌	┌	
loading type	I	II	III	I	I	I	II	II	II	II	
concrete compressive strength	28.3 MPa				30.4 MPa		28.3 MPa		30.4 MPa		
beams	cross section	300 x 300 mm									
	span	2700 mm									
	longitudinal reinforcement	8+8-D13 (SD390) $a_t = 868 \text{ mm}^2$				6+6-D16 (SD345) $a_t = 902 \text{ mm}^2$		10+10-D13 (SD390) $a_t = 1122 \text{ mm}^2$		6+6-D16 (SD345) $a_t = 902 \text{ mm}^2$	
	anchorage length	N/A							300	258	159
	stirrups	D6 stirrup @ 50 mm (SD295)									
columns	cross section	300 x 300 mm									
	span	1470 mm									
	longitudinal reinforcement	16-D13 (SD345) $a_g = 2032 \text{ mm}^2$				14-D13 (SD345) $a_g = 1778 \text{ mm}^2$		8-D13 (SD345) $a_g = 954 \text{ mm}^2$		6-D13 (SD345) $a_g = 696 \text{ mm}^2$	
	hoops	D6 hoop @ 50 mm (SD295)									
joint	hoops	D6 square hoops x 3 sets (SD295)									
	transverse beams	section	N/A			300 x 300 mm	N/A				
longitudinal reinforcement					16-D13						
axial load	216 kN										

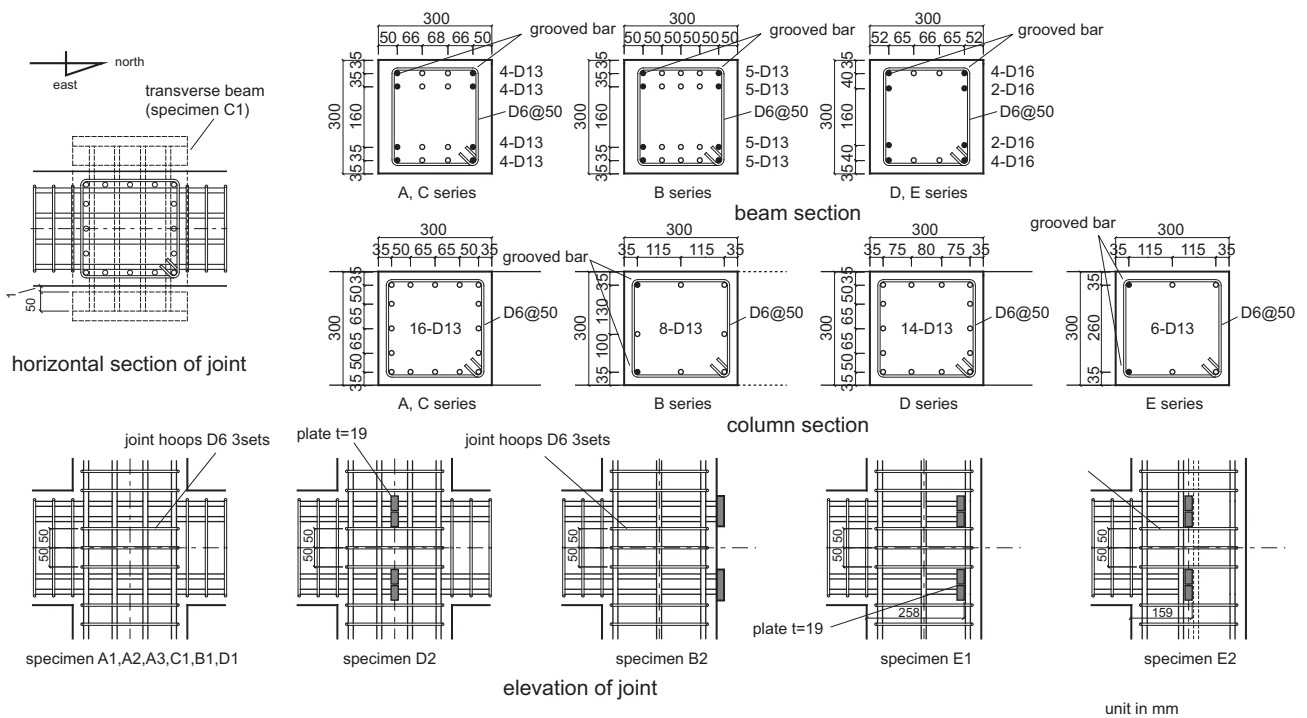


Figure 1 Geometry and reinforcing details of specimens

2.2. Materials

Normal portland cement concrete with design compressive strength of 24 MPa was used. The average compressive strength of the concrete by cylinder test were 28.3 MPa for test series A, B and C and 30.4 MPa for test series D and E respectively.

The D13 of SD390 grade and D16 of SD345 grade deformed bars were used for longitudinal bars in beams while the D13 bars of SD345 grade were used for columns. The D6 deformed bars of SD295 grade were used for transverse reinforcement in joints, beams and columns. The mechanical properties of the concrete and the bars are listed in Table 2 and Table 3.

Table 2 Mechanical properties of concrete

Test series	compressive strength, MPa	Young's modulus, GPa	tensile splitting strength, MPa
A, B, C	28.3	25.9	2.67
D, E	30.4	30.0	2.90

Table 3 Mechanical properties of bars

Test series	Reinforcing Bars	Young's modulus, GPa	yield strength, MPa	tensile strength, MPa	
A,B,C	beams	D13(SD390)	176	456	582
	columns	D13(SD345)	176	357	493
	hoops and stirrups	D6(SD295)	151	326	488
D,E	beams	D16(SD345)	187	379	558
	columns	D13(SD345)	187	375	538
	hoops and stirrups	D6(SD295)	191	366	504

2.3. Test setup and loading sequence

Figure 2 shows the different loading methods and the boundary conditions for namely loading types I, II and III. Loading type I simulates a typical boundary condition of an interior beam-column joint subjected to lateral load (Fig. 2 (a)). Loading type II simulates a typical boundary condition of an exterior beam-column joint (Fig. 2 (b)). No internal stress occurred in the free beam which is not supported even if the specimen has crucial form like specimen A2. Loading type III simulates a boundary condition of a corner joint (Fig. 2 (c)). The end of the no-loaded beam is free and the top of the upper column is free in horizontal direction. Therefore no internal

force is acted in the free beam and only axial load acted in the upper column.

In the case of loading type I and II, statically cyclic lateral load was applied at the top of the column by displacement control with a horizontal servo controlled actuator with capacity of 200 kN. In the test of specimen A3, in which the loading type III is used, a 500 kN horizontal hydraulic jack connecting a reaction frame and the end of the beam is used to apply a horizontal load. The load history is shown in Fig. 3. In all the specimens, constant compressive axial load of 216kN is applied before lateral loading by a 500kN vertical servo controlled hydraulic actuator.

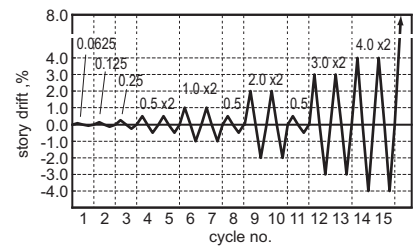


Figure 3 Loading history

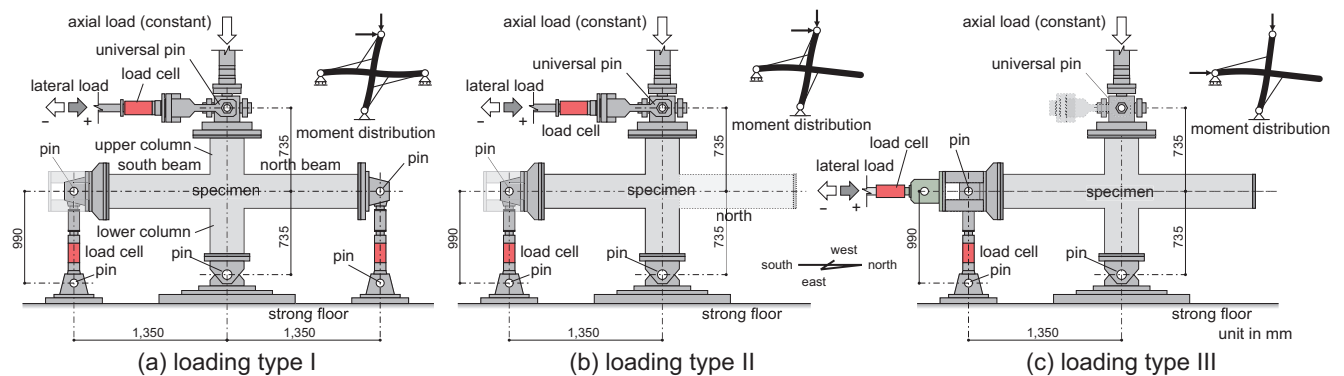


Figure 2 Loading setup

2.4 Instrumentation

Major instrumentation includes, (1) story shear, (2) story drift ratio, (3) beam deflection, (4) column deflection, (5) joint deformation as well as (6) stresses and strains in reinforcing bars. The instrumentations proposed by the authors (Kusuhara 2006) were used to measure joint deformations and stresses in reinforcing bars.

To measure the stresses in the bars after yielding, box shape grooves were made on the two sides of each deformed bar (See Photo 1) to get reduced section. The sectional area of the bars was reduced by almost 30 % along the length except the locations where strain gauges were placed, such that reinforcing bars should not yield and remain in linearly elastic range adjacent to the strain gauges and the stresses of bars were calculated from sectional area, Young's modulus and the strains.

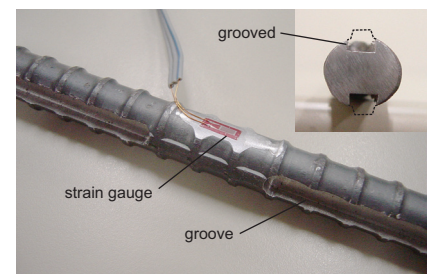


Photo 1 Grooved bar

3. TEST RESULTS AND DISCUSSION

3.1. Development of cracks

The observed cracking pattern in the joint of each specimen at story drift of 4 % is shown in Fig. 4. As the joint of Specimen C1 is covered with transverse beams no crack pattern is shown. In all the specimens the flexural cracks at the beam ends started at the corner and propagated to the direction of center of the beam-column joint diagonally. The diagonal cracks in beam-column joints grew toward the ends of beam bars and extended to the column regions in the specimen E1 and E2, where the beam bars were anchored with heading bars in the joints. Concrete cover did not spall off on the beam-column joints before story drift ratio of 2% and the cover concrete started spalling off at the load cycle of 3% story drift or more primarily on the beam-column joint for Specimens A1 and specimens of B, D and E series and on the beam end for Specimen A2 and A3 respectively.

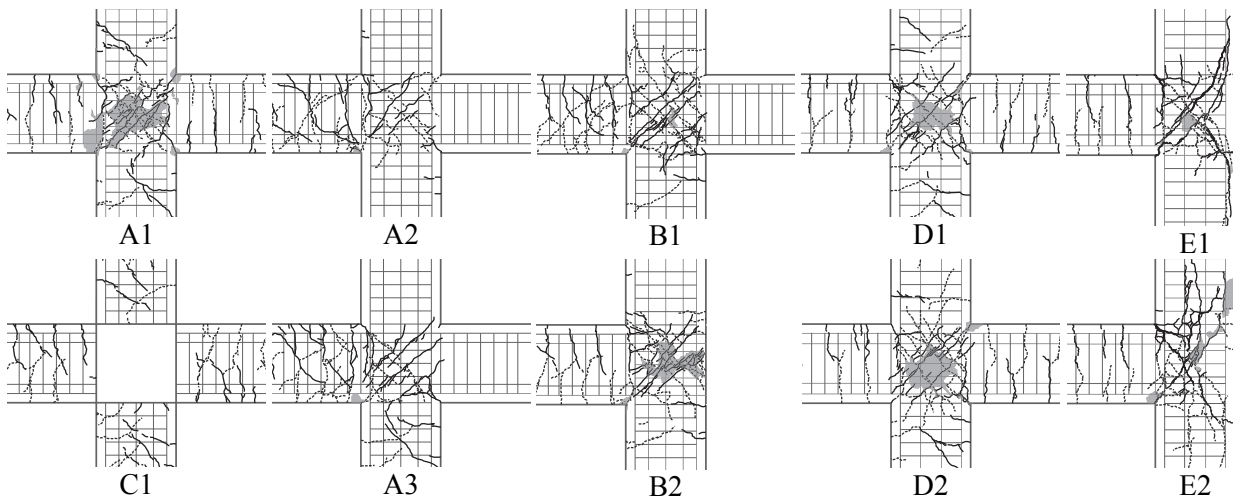


Figure 4 Observed crack pattern at 4% story drift

3.2. Story shear-story drift relation

The story shear-story drift ratio relations are plotted in Fig. 5. In all the specimens the beam bars in the first layer yielded at story drift of 0.8% through 1.5%. Although calculated story shear of column yielding are over 25 percent higher than that of the beam yielding, column bars also yielded except for Specimen A2. What is more, the column bars of Specimen E2, which has poor anchorage length of beam bars, yielded at 52% of predicted story shear of column yielding before the beam yielded.

The shape of the hysteresis loops of all the specimens loaded with loading type I are pinched. The maximum story shear of Specimen C1, which has transverse beams, is approximately 20% higher than that of Specimen A1. The maximum story shear and the shapes of the hysteresis loops of Specimen D1 and D2, with or without anchor plates, are very similar to each other. The maximum story shear of Specimens B1 and B2 is close each other. But Specimen B2 showed severer strength degradation after load reversals than Specimen B1. When Specimen E2 compared with Specimen E1, poor anchorage length of beam bars leads yielding of column bars and 12 % lower capacity of story shear. Obviously the envelope curve of Specimen A3 is not symmetric.

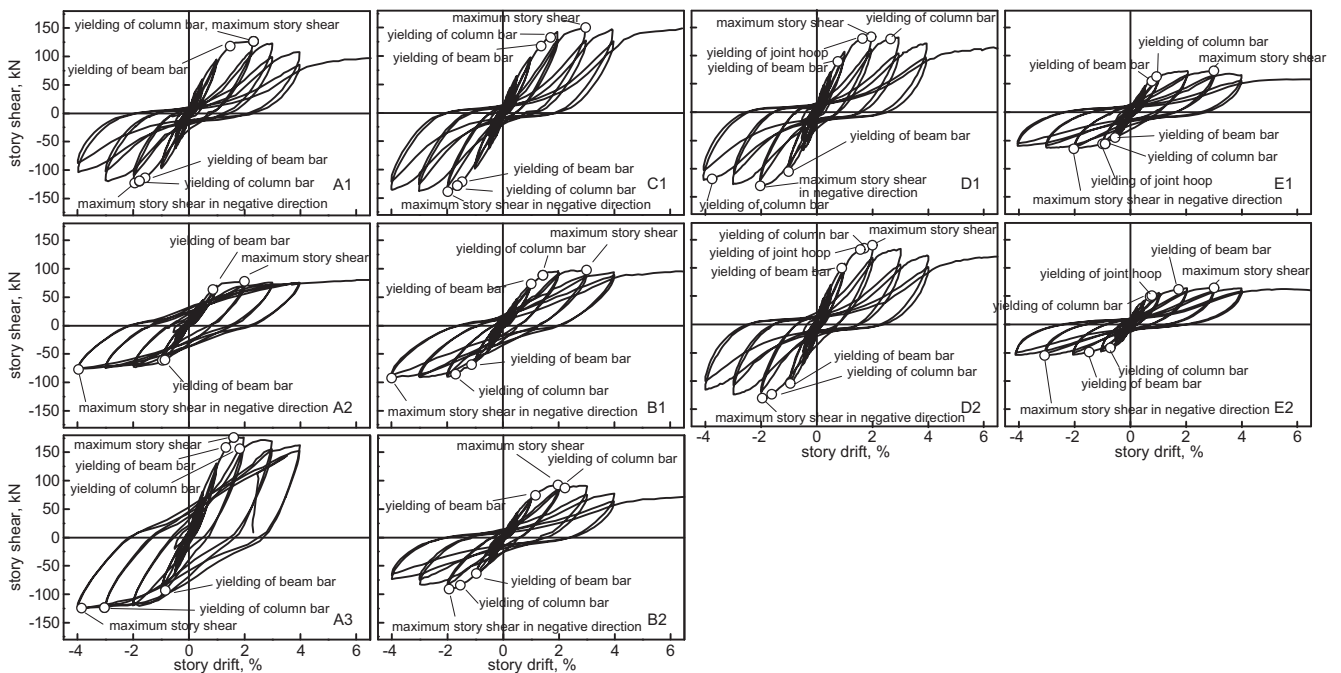


Figure 5 Story shear - story drift ratio relations

lateral capacity in the positive direction (or closing direction) is more than 40% higher than that in the negative direction (or opening direction).

Specimen A2 and A3, of which damage on joints are not so severe, show relatively stable and fat hysteresis loops while the other specimens show pinched hysteresis loops with less energy dissipation.

3.3. Predicted and observed strength

Story shear at flexural yield and ultimate strengths of the beam and the column were calculated by the flexural theory using the mechanical properties of the materials. The observed strengths at the first beam yield were smaller than that calculated by flexural theory except for Specimen A2 and A3, which have relatively stable and fat hysteresis loops. The observed strengths at the column yield were much smaller than that calculated by the flexural theory in all the specimens but Specimen A2 in which no yield of column bars were observed. The observed maximum strengths are almost equal to the predicted story shear at ultimate strength of the beam except those Specimen A1 and E2.

Though the longitudinal bars on the first and the second layer yielded at attained maximum story shear at story drift of 2.0% before severe damage in the joint region occurred after story drift of 3.0%, the observed maximum story shear of specimen A1 was through 7 % to 9 % smaller than calculated.

Table 4 Predicted and observed story shear

		A1	C1	A2	A3	B1	B2	D1	D2	E1	E2
story shear at yielding of beam bars at first layer ,kN	calculated	120.7		60.4	142.2 -104.1	76.4		113.2		56.6	
	observed	118.6	117.8	63.3	158.3 -93.4	73.6	74.5	89.7	99.7	54.9	48.6
observed story shear / calculated story shear		0.98	0.98	1.05	1.11 0.90	0.96	0.97	0.79	0.88	0.97	0.86
story shear at yielding of column bars at first layer ,kN	calculated	154.5		169.3 -143.0	168.4 142.2	110.4 -91.7		151.5		95.0 -78.4	
	observed	126.6	132.7	-	156.1 -123.6	88.9 -85.4	87.2 -84.2	129.4	123.4	63.1 -56.1	49.4 -41.7
observed story shear / calculated story shear		0.82	0.86	N/A	0.93 0.87	0.81 0.93	0.79 0.92	0.78	0.81	0.66 0.72	0.52 0.53
calculated story shear ,kN	(1) at ultimate strength of beam	136.3		68.1	159.1 -118.6	85.6		125.3		62.7	
	(2) at ultimate strength of column	179.8		194.2 -166.8	195.0 -166.0	127.9 -106.2		175.2		112.8 -92.8	
observed maximum story shear ,kN		126.6 -122.8	150.3 -139.0	77.9 -77.1	176.4 -124.5	98.4 -92.6	92.2 -91.1	133.9 -130.5	140.2 -130.5	73.2 -64.8	65.0 -55.0
observed story shear / calculated story shear (1)		0.93 0.91	1.10 1.02	1.14 1.13	1.11 1.05	1.15 1.08	1.08 1.06	1.07 1.04	1.12 1.04	1.17 1.03	1.04 0.88

3.5. Subcomponents of deformation

Figure 7 shows the subcomponents of the deformation (Kusuhara 2006) observed in the tests of Specimen A1 and A2, which have identical geometry and bar arrangement but used different loading type. The components include (a) chord rotation of beams R_b , (b) chord rotation of columns R_c , (c) rigid rotation at beam ends e_θ , (d) face rotation of joint panel p_θ and (e) shear strain in joint panel γ_p . (see Figure 6)

In Specimen A1, which simulated an interior beam-column joint and of which damage in joint concrete was severe, the face rotation of joint panel and shear strain of joint panel are dominant

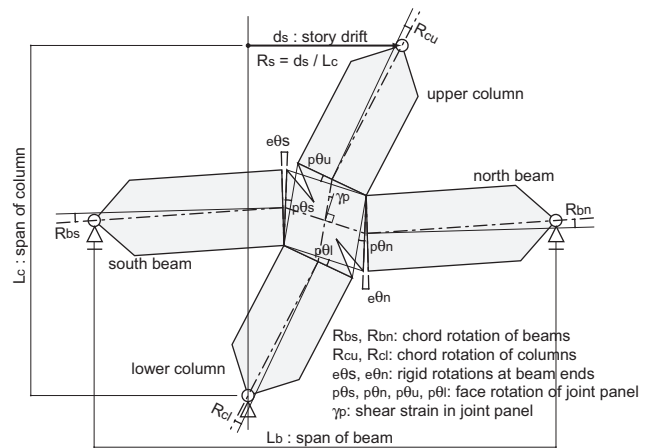


Figure 6 Definition of subcomponents of deformation

components. The face rotations of joint panel at beam side are less than the chord rotation of beams at early load cycles. Once longitudinal bars in the beams yielded, the face rotation of joint panel suddenly increased. On the contrary, the chord rotations of beams and rigid rotations at beam ends seemed to keep elastic even after the beam bars yielded.

In Specimen A2, which simulated an exterior beam-column joint and of which joint concrete damaged slightly, the rigid rotation of south beam was dominant in particular the specimen was loaded to positive direction whereas the chord rotation of south beam was dominant when it was loaded to negative direction. The rigid rotation of the north beam end was very small and negligible.

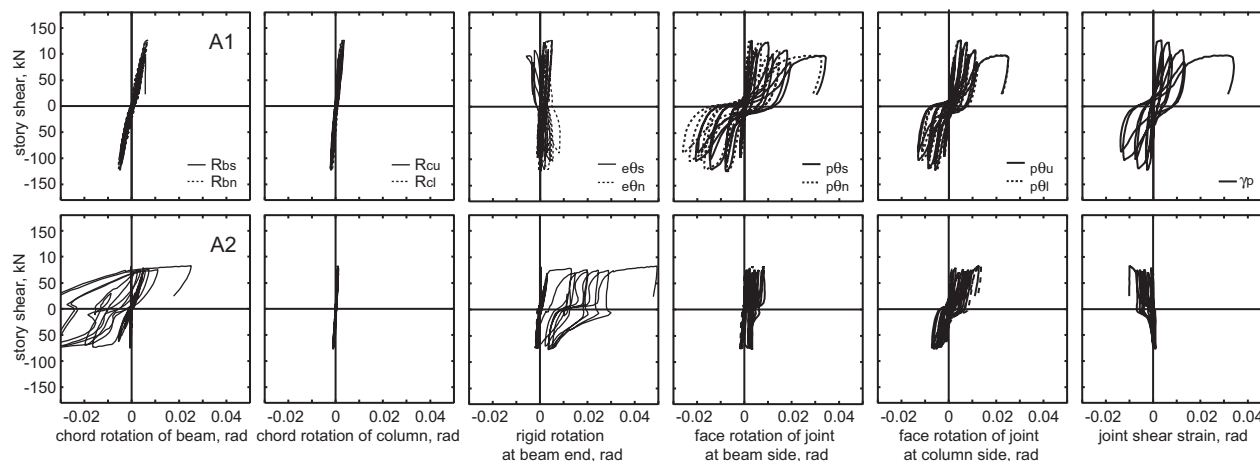


Figure 7 Subcomponents of the deformation

3.4. Stress distribution at beam end and bond stress on beam longitudinal bars passing through the joint

Figure 8 shows the distribution of stress at the ends of the south beams measured with the grooved bars for Specimen A1, C1, D1, D2, A2 and E1. In the specimens tested under condition of interior joint, the stress in compressive reinforcement shifted to tension after the story drift of 0.5%. In particular on the third layer (second layer of compressive reinforcement) large tension stress was attained and it approximately reached the yield stress. Furthermore, in Specimen E1, which simulated exterior joint and was damaged in the joint, tension shift of compressive bars were observed in spite of the bars which were not in tension at the opposite side of the joint.

On the contrary, in Specimen A2, which showed typical behavior of beam yielding, the stress distribution in longitudinal bars at beam end changes linearly in the section.

Figure 9 shows the envelope curve of average bond stress on beam bar vs. story drift ratio relationships for specimens used loading type I. The bond force was calculated based on the stress measured with the grooved bars. In Specimen A1, the bond stress reached its maximum value around story drift of 1 % before the story shear attained its maximum value. In Specimen C1, D1 and D2, the bond force reached its maximum value around story drift of 3 % and it decreased as the story drift was increased. Maximum bond stress of the second layer is around 40% to 60% of the maximum bond stress of the first layer.

Considering the nominal bond capacities of beam bars in beam-column joint calculated by the AIJ Guidelines, which are 7.2 MPa for Specimen A1 and C1 and 7.4 MPa for Specimen D1 respectively, the test result reached only through 50 % to 80 % of the calculated nominal strength.

As the observed bond stress were not reached the calculated strength and it decreased even in Specimen D2, which has anchor plates in the joint, the degradation of bond stress on beam bars and the tension shift of compressive reinforcements are not due to the bond failure. It should be caused by increasing of tension strain in the bars due to the opening of diagonal cracks in beam-column joint. All the more, the bond stress of second

layer is smaller because the diagonal cracks open widely at the center of the joints.

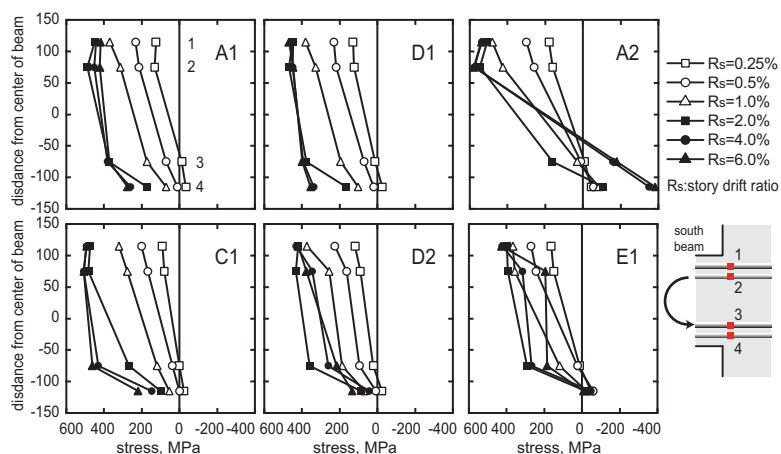


Figure 8 Stress in beam bars at end of south beam

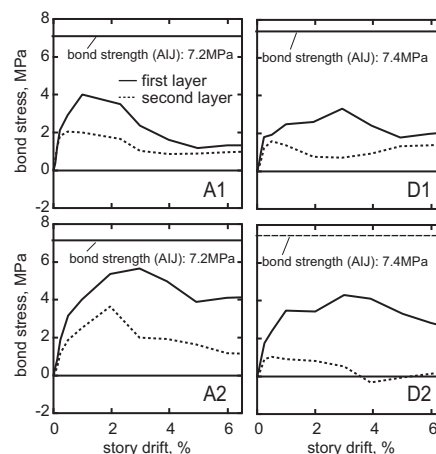


Figure 9 Bond stress in beam bars passing the joint

4. CONCLUDING REMARKS

The followings are brief summaries of the test results.

- (1) In some case of damage of the joints were severe, maximum story shear was lower than predicted story shear at ultimate strength of beam in spite of beam bars yielded.
- (2) The test results indicated that the rotations of the four parts of the joint divided with diagonal cracks were dominant in the story drift deformation in case of the joint failed after yielding of the beams.
- (3) The deflection of the beams and the rotations at the beam ends were dominant in case of damage on the joints were minor and showed relatively stable and fat hysteresis loop of the story shear vs. story drift relation.
- (4) The story shear capacity of the specimen with transverse beams, in which the damage of the joint was severe, was improved.
- (5) In case of damage of joints were severe, bond actions of beam bars passing through the joints kept lower level than the bond strength specified in the AIJ Guideline.
- (6) Poor anchorage length of beam bars in exterior joints led lower story shear capacity, yielding of column bars and severe damage in the joint.

ACKNOWLEDGMENTS

The tests were partially supported by the Grants-in-Aid for Scientific Research (B), FY 2003-2004, Grant No. 15360291, Principal Investigator: Hitoshi Shiohara, Japan Society for the Promotion of Science.

REFERENCES

- Architectural Institute of Japan (1999), Design Guidelines for Earthquake Resistant Reinforced Concrete Building Based on Inelastic Displacement Concept, Architectural Institute of Japan, Tokyo, Japan, 440 pp. (in Japanese)
- Kusuhara, F. and H. Shiohara (2006), New Instrumentation for Damage and Stress in Reinforced Concrete Beam-Column Joint, *Proc. of the 8NCEE*, April 18-22, 2006, San Francisco, California, USA, Paper No. 1214 (CD-ROM).